



## Letter

Effect of  $\text{Li}_{0.12}\text{Na}_{0.88}\text{NbO}_3$  content on the electrical properties of  $\text{Bi}_{0.50}\text{Na}_{0.50}\text{TiO}_3$  lead-free piezoelectric ceramics

Tao Chen\*, Ting Zhang, Guangchang Wang, Jifang Zhou, Jianwei Zhang, Yuhong Liu

Teaching and Research Section of Physics, Chengdu Medical College, Chengdu 610083, PR China

## ARTICLE INFO

## Article history:

Received 24 November 2011

Received in revised form

30 December 2011

Accepted 2 January 2012

Available online 14 January 2012

## Keywords:

 $\text{Bi}_{0.50}\text{Na}_{0.50}\text{TiO}_3$  $\text{Li}_{0.12}\text{Na}_{0.88}\text{NbO}_3$ 

Electrical properties

## ABSTRACT

$\text{Li}_{0.12}\text{Na}_{0.88}\text{NbO}_3$ -modified  $\text{Bi}_{0.50}\text{Na}_{0.50}\text{TiO}_3$  [(1-x)BNT-xLNN] lead-free piezoelectric ceramics were prepared by the conventional solid-state solid method. Effects of LNN content on the electrical properties of (1-x)BNT-xLNN ceramics were investigated. The relaxor behavior of (1-x)BNT-xLNN ceramics gradually enhances, and the depolarization temperature decreases with increasing LNN content. The largest  $\epsilon_m$  value and the lowest dielectric loss are demonstrated for the ceramic with  $x=0.02$ . Moreover, the (1-x)BNT-xLNN ceramic with  $x=0.02$  also has an enhanced piezoelectric behavior of  $d_{33} \sim 113$  pC/N and  $k_p \sim 21.6\%$ . Therefore, the introduction of LNN could be an effective way to improve the electrical behavior of BNT ceramics.

© 2012 Elsevier B.V. All rights reserved.

## 1. Introduction

Ferroelectric ceramics have been widely used in the field of microelectronic and microelectromechanical devices because of their good dielectric, ferroelectric, pyroelectric, and piezoelectric properties. However, some environmental issues have restricted some applications of lead-based ferroelectric ceramics because of their toxicity and high vapor pressure during processing and preparation [1]. Therefore, lead-free ceramics have been given considerable attention [2–6]. In 1960, sodium bismuth titanate ( $\text{Bi}_{0.50}\text{Na}_{0.50}\text{TiO}_3$ , BNT) was first found by Smolenskii and Aganovskaya [7]. Recently, considerable attention has been given to these BNT-based ceramics for the replacement of lead-based piezoelectric ceramics.

BNT-based ceramics have been considered a promising candidate of lead-free piezoelectric ceramics because of its strong ferroelectricity and a high Curie temperature of  $\sim 320^\circ\text{C}$  [8–13]. However, some shortcomings seriously hinder the development and practical application of BNT-based ceramics [8–13], for example, a large coercive field and a high conductivity. In the past, some attempts have been used to resolve these issues of BNT-based ceramics. Among these, the formation of BNT solid solutions with other ferroelectrics is to help improve their electrical properties, for example, BNT-BaTiO<sub>3</sub> [14], BNT-K<sub>0.5</sub>Bi<sub>0.5</sub>TiO<sub>3</sub> [15], BNT-KNbO<sub>3</sub> [16], and Bi(Mg<sub>2/3</sub>Nb<sub>1/3</sub>)O<sub>3</sub> [17]. Although their piezoelectric properties were improved, the dielectric loss of these materials is often

high [18,19]. A solid solution of ( $\text{Li}_{0.12}\text{Na}_{0.88}$ )NbO<sub>3</sub> (LNN) has been considered as a promising candidate for the high-frequency filter application [20–25]. Moreover, a low dielectric loss is also observed for such a LNN material [25]. Therefore, it is expected that a high piezoelectric constant and a low dielectric loss of BNT ceramics are induced by introducing the LNN.

In the paper, (1-x) $\text{Bi}_{0.50}\text{Na}_{0.50}\text{TiO}_3$ -x $\text{Li}_{0.12}\text{Na}_{0.88}\text{NbO}_3$  [(1-x)BNT-xLNN] lead-free piezoelectric ceramics were prepared by the conventional solid-state solid method, and effects of LNN content on the electrical properties of (1-x)BNT-xLNN ceramics were investigated. Enhanced piezoelectric properties have been observed for these BNT ceramics doped with optimum LNN content, together with a low dielectric loss. Underlying physical mechanisms are also addressed.

## 2. Experiments

(1-x)BNT-xLNN lead-free piezoelectric ceramics with  $x=0$ –0.08 were fabricated by using the conventional solid state reaction method. In this work, raw materials were Na<sub>2</sub>CO<sub>3</sub> (99.8%), Nb<sub>2</sub>O<sub>5</sub> (99.5%), Bi<sub>2</sub>O<sub>3</sub> (99%), Li<sub>2</sub>CO<sub>3</sub> (99.99%), and TiO<sub>2</sub> (99%). All raw materials were weighed according to the stoichiometric ratio of (1-x)BNT-xLNN, ball mixed in the alcohol, dried in an oven at 80 °C, and then calcined at 850 °C for 6 h. These calcined mixtures were again ball milled and then pressed into the pellet disk of  $\sim 1.5$  cm diameter and  $\sim 1.0$ –1.2 mm thickness. All samples were sintered in air at the same temperature of  $\sim 1160^\circ\text{C}$  for 2 h by using the crucibles without any atmospheric powder. They were coated with silver on both sides of all ceramics and annealed at 800 °C for 30 min in order to characterize their electrical properties. The x-ray diffraction (XRD) machine was used to characterize the phase structure of all sintered pellets. The temperature dependence of the dielectric constant of all ceramics was investigated in the temperature range of 25–500 °C by using a programmable furnace with an LCR analyzer (TH2816). A poling process was conducted in the silicon oil by using a dc power supply under  $\sim 6.0$  kV/mm for 20 min at room temperature. The  $d_{33}$  value of these ceramics was

\* Corresponding author.

E-mail addresses: [chentaocmc@163.com](mailto:chentaocmc@163.com), [myfriendsroom@163.com](mailto:myfriendsroom@163.com) (T. Chen).

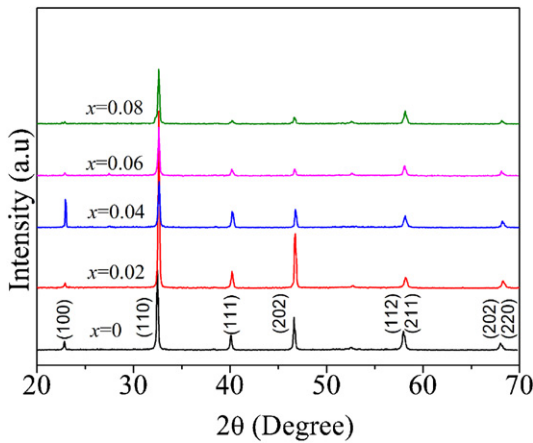


**Fig. 1.** XRD patterns of  $(1-x)\text{Bi}_{0.50}\text{Na}_{0.50}\text{TiO}_3-x\text{Li}_{0.12}\text{Na}_{0.88}\text{NbO}_3$  ceramics as a function of LNN content.

measured using a piezo- $d_{33}$  meter (ZJ-3A, China), and their  $k_p$  values were calculated from the measured resonance-antiresonance frequencies using an Agilent 4294A precision impedance analyzer.

### 3. Results and discussion

XRD patterns of these  $(1-x)\text{BNT}-x\text{LNN}$  ceramics were measured, as shown in Fig. 1. A pure perovskite structure is identified, and no secondary phases can be observed for all ceramics in this work, confirming that the LNN has diffused into the BNT lattice during sintering. The feature peak located at  $\sim 47^\circ$  does not split for all ceramics, indicating that a rhombohedral symmetry structure is involved into these  $(1-x)\text{BNT}-x\text{LNN}$  ceramics. Similar phenomenon has been observed for the BNT-based ceramics [26,27]. However, it is also observed from Fig. 1 that a higher intensity of XRD peaks is only demonstrated for the  $(1-x)\text{BNT}-x\text{LNN}$  ceramic with  $x=0.02$ . Therefore, the introduction of optimum LNN

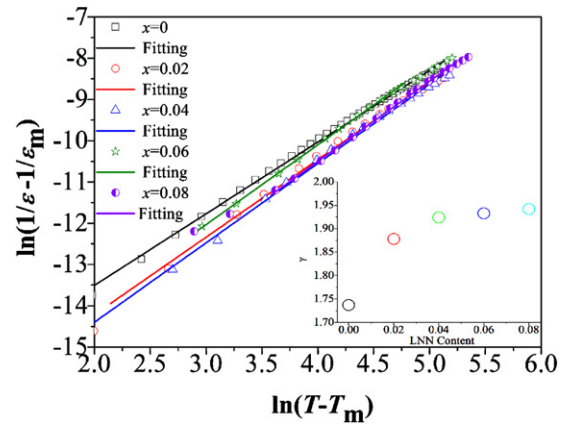


**Fig. 3.**  $\ln(1/\varepsilon - 1/\varepsilon_m)$  vs.  $\ln(T - T_m)$  curves for  $(1-x)\text{Bi}_{0.50}\text{Na}_{0.50}\text{TiO}_3-x\text{Li}_{0.12}\text{Na}_{0.88}\text{NbO}_3$  ceramics, and the insert is the  $\gamma$  value as a function of LNN content.

content may lead to the improvement of the crystalline property of BNT ceramics.

Fig. 2(a)–(e) shows the temperature dependence of the dielectric constant ( $\varepsilon_r$ ) of  $(1-x)\text{BNT}-x\text{LNN}$  ceramics, measured at 1–1000 kHz. These peaks of the dielectric constant vs. temperature become much broader with increasing LNN content in these ceramics, as shown in Fig. 2(a)–(e). The diffuseness of the phase transition of these ceramics can be defined by the modified Curie-Weiss law, as described in Eq. (1).

$$\frac{1}{\varepsilon_r} - \frac{1}{\varepsilon_m} = C^{-1}(T - T_m)^\gamma \quad (1)$$

where  $\varepsilon_m$  is the maximum value of  $\varepsilon_r$  at the phase transition temperature of  $T_m$ ,  $\gamma$  is the degree of diffuseness, and  $C$  is the Curie-like constant. The nature of the phase transition can be identified by the  $\gamma$  value. It is well known that a  $\gamma$  value of 1 is a normal ferroelectric and  $\gamma=2$  is for an ideal ferroelectric relaxor. Fig. 3 indicates

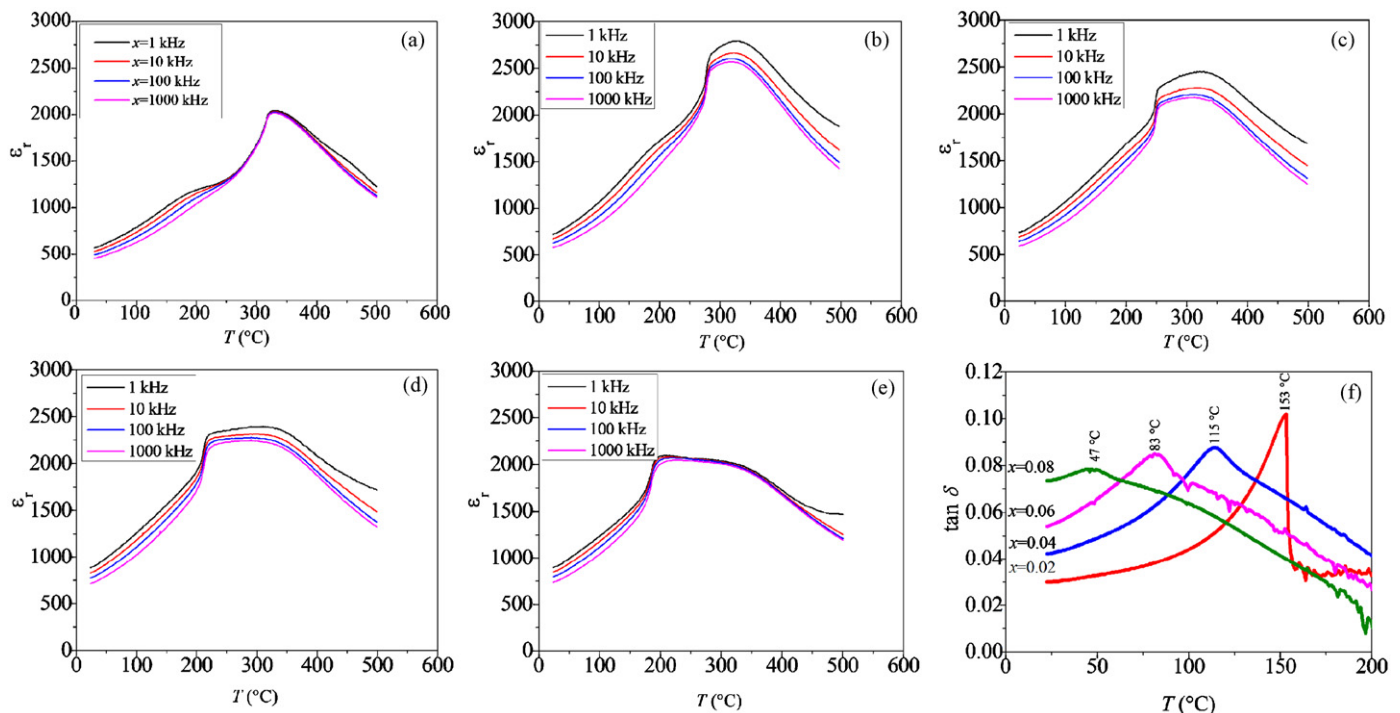


**Fig. 2.** Temperature dependence of the dielectric constant of  $(1-x)\text{Bi}_{0.50}\text{Na}_{0.50}\text{TiO}_3-x\text{Li}_{0.12}\text{Na}_{0.88}\text{NbO}_3$  ceramics: (a)  $x=0$ , (b)  $x=0.02$ , (c)  $x=0.04$ , (d)  $x=0.06$ , (e)  $x=0.08$ , and (f) temperature dependence of the dielectric loss of  $(1-x)\text{Bi}_{0.50}\text{Na}_{0.50}\text{TiO}_3-x\text{Li}_{0.12}\text{Na}_{0.88}\text{NbO}_3$  ceramics, measured at 100 kHz.

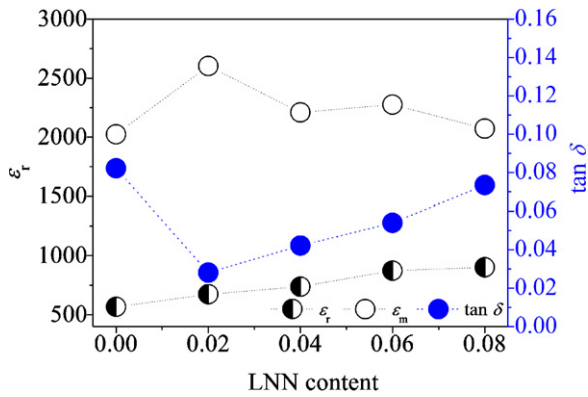


Fig. 4. Dielectric properties of  $(1-x)\text{Bi}_{0.50}\text{Na}_{0.50}\text{TiO}_3-x\text{Li}_{0.12}\text{Na}_{0.88}\text{NbO}_3$  ceramics.

$\ln(1/\epsilon_r - 1/\epsilon_m)$  vs.  $\ln(T - T_m)$  at 100 kHz for the  $(1-x)\text{BNT}-x\text{LNN}$  ceramics. All ceramics have a linear relationship for the plots of  $\ln(1/\epsilon_r - 1/\epsilon_m)$  vs.  $\ln(T - T_m)$ . The  $\gamma$  value can be determined by the least-squared fitting the experimental data according to the Eq. (1). The insert of Fig. 3 plots the  $\gamma$  value vs. LNN content of  $(1-x)\text{BNT}-x\text{LNN}$  ceramics. The  $\gamma$  value of  $(1-x)\text{BNT}-x\text{LNN}$  ceramics gradually increases from  $\sim 1.737$  to  $\sim 1.942$  with increasing LNN content, that is, the relaxor behavior of  $(1-x)\text{BNT}-x\text{LNN}$  ceramics gradually becomes much stronger. As compared with normal ferroelectrics, the dynamic polar nanometer-sized regions (PNRs) appear in relaxor ferroelectrics. The local electric fields and elastic fields give rise to the PNRs, by hindering the long-range dipole alignment. For the  $(1-x)\text{BNT}-x\text{LNN}$  ceramics, the ionic radii of  $\text{Nb}^{5+}/(\text{Li}, \text{Na})^+$  is respectively different from that of  $\text{Ti}^{4+}/(\text{Bi}, \text{Na})^{2+}$ , together with their different valences. Therefore, the relaxor behavior in  $(1-x)\text{BNT}-x\text{LNN}$  ceramics should be attributed to the cationic disorder induced by the LNN substitutions for BNT. Fig. 2(f) shows the temperature dependence of the dielectric loss of  $(1-x)\text{BNT}-x\text{LNN}$  ceramics, measured at 100 kHz. As shown in Fig. 2(f), a peak of the dielectric loss is observed for all ceramics in this work. Usually, the depolarization temperature ( $T_d$ ) could be determined by the temperature dependence of the dielectric loss in these BNT-based piezoelectric ceramics [28,29]. Therefore, these peaks for the temperature dependence of the dielectric loss can characterize the  $T_d$  value in this work. Moreover, it was observed from Fig. 2(f) that the  $T_d$  value of  $(1-x)\text{BNT}-x\text{LNN}$  ceramics decreases with increasing LNN content.

Fig. 4 shows the dielectric properties of  $(1-x)\text{BNT}-x\text{LNN}$  ceramics as a function of LNN content, measured at 100 kHz and room temperature. As shown in Fig. 4, the  $\epsilon_r$  value of  $(1-x)\text{BNT}-x\text{LNN}$  ceramics gradually increases with increasing LNN content. However, the  $(1-x)\text{BNT}-x\text{LNN}$  ceramic with  $x=0.02$  has the highest  $\epsilon_m$  value. Moreover, the dielectric loss ( $\tan \delta$ ) of  $(1-x)\text{BNT}-x\text{LNN}$  ceramics firstly decreases dramatically with increasing LNN content, reaches a minimum value for  $x=0.02$ , and then gradually increases with increasing LNN content. Therefore, the  $(1-x)\text{BNT}-x\text{LNN}$  ceramic with  $x=0.02$  demonstrates an enhanced dielectric behavior of a low  $\tan \delta$  value and a large  $\epsilon_m$  value.

Fig. 5 plots the piezoelectric properties and the mechanical quality factor ( $Q_m$ ) of  $(1-x)\text{BNT}-x\text{LNN}$  ceramics as a function of LNN content. The  $d_{33}$  value of  $(1-x)\text{BNT}-x\text{LNN}$  piezoelectric ceramics increases with increasing LNN content, reaches a maximum value of  $\sim 113$  pC/N at  $x=0.02$ , and gradually decreases with further increasing LNN content. Similar to the  $d_{33}$  value, the  $(1-x)\text{BNT}-x\text{LNN}$  ceramic with  $x=0.02$  has a highest  $k_p$  value of  $\sim 21.6\%$  among these ceramics. However, the  $Q_m$  value of  $(1-x)\text{BNT}-x\text{LNN}$  ceramics gradually increase with increasing LNN content because of the LNN material with a high  $Q_m$  value [25]. In this work, the enhancement

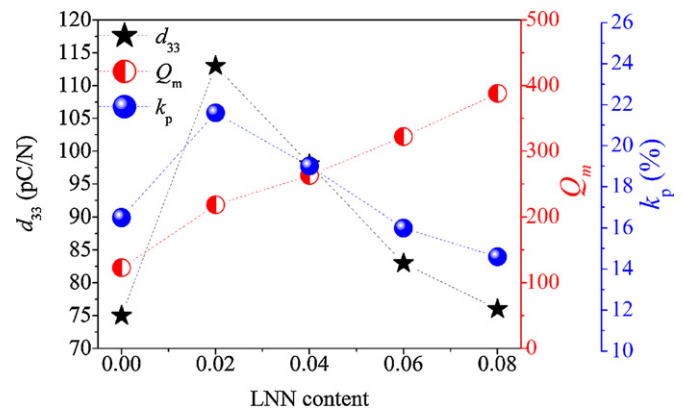


Fig. 5. Piezoelectric properties and mechanical quality factor of  $(1-x)\text{Bi}_{0.50}\text{Na}_{0.50}\text{TiO}_3-x\text{Li}_{0.12}\text{Na}_{0.88}\text{NbO}_3$  ceramics.

in piezoelectric properties should be attributed to the introduction of an optimum LNN content, where the intensity of XRD peaks is improved greatly for the ceramic with  $x=0.02$ .

#### 4. Conclusions

$(1-x)\text{Bi}_{0.50}\text{Na}_{0.50}\text{TiO}_3-x\text{Li}_{0.12}\text{Na}_{0.88}\text{NbO}_3$  lead-free piezoelectric ceramics were prepared by the conventional solid-state method, and the LNN content strongly affects the electrical properties of  $(1-x)\text{BNT}-x\text{LNN}$  ceramics. The introduction of LNN enhances the relaxor behavior of  $(1-x)\text{BNT}-x\text{LNN}$  ceramics. A larger  $\epsilon_m$  value and a lower  $\tan \delta$  value have been demonstrated for these LNN-modified BNT ceramic with  $x=0.02$ . Moreover, improved piezoelectric properties are observed for the 2% LNN-modified BNT ceramics. Therefore, optimizing the LNN content is an effective way to enhance the piezoelectric properties of BNT ceramics.

#### Acknowledgment

Authors gratefully acknowledge the supports of the Chengdu Medical College.

#### References

- [1] P.K. Panda, J. Mater. Sci. 44 (2009) 5049.
- [2] J.G. Wu, Y.Y. Wang, D.Q. Xiao, J.G. Zhu, Appl. Phys. Lett. 91 (2007) 132914.
- [3] Y. Saito, H. Takao, T. Tani, T. Nonoyama, K. Takatori, T. Homma, T. Nagaya, M. Nakamura, Nature 432 (2004) 84.
- [4] J. Wu, D. Xiao, W. Wu, J. Zhu, J. Wang, J. Alloys Compd. 509 (2011) L359.
- [5] W.F. Liu, X.B. Ren, Phys. Rev. Lett. 103 (2009) 257602.
- [6] J. Wu, D. Xiao, W. Wu, Q. Chen, J. Zhu, Z. Yang, J. Wang, Scripta Mater. 65 (2011) 771.
- [7] G.A. Smolenskii, A.I. Aganovskaya, Sov. Phys. Solid State 1 (1960) 1429.
- [8] J. Suchanik, Ferroelectrics 165 (1995) 249.
- [9] S.D. Said, J.P. Mercurio, J. Eur. Ceram. Soc. 21 (2001) 1333.
- [10] X.X. Wang, K.W. Kwok, X.G. Tang, H.L.W. Chan, C.L. Choy, Solid State Commun. 129 (2004) 319.
- [11] T. Takenaka, K.I. Maruyama, K. Sakata, Jpn. J. Appl. Phys. 30 (1991) 2236.
- [12] Z.P. Yang, B. Liu, L.L. Wei, Y.T. Hou, Mater. Res. Bull. 43 (2008) 81.
- [13] T. Takenaka, T. Okuda, K. Takegahara, Ferroelectrics 196 (1997) 175.
- [14] Y. Bai, G.P. Zheng, S.Q. Shi, Mater. Res. Bull. 46 (2011) 1866.
- [15] Y.M. Li, W. Chen, J. Zhou, Q. Xu, H.J. Sun, M.S. Liao, Ceram. Int. 31 (2005) 139.
- [16] G. Fan, W. Lu, X. Wang, F. Liang, J. Xiao, J. Phys. D: Appl. Phys. 41 (2008) 035403.
- [17] C.R. Zhou, X.Y. Liu, J. Mater. Sci. 43 (2008) 1016.
- [18] H. Ni, L. Luo, W. Li, Y. Zhu, H. Luo, J. Alloys Compd. 509 (2011) 3958.
- [19] X.X. Wang, S.H. Choy, X.G. Tang, H.L.W. Chan, J. Appl. Phys. 97 (2005) 104101.
- [20] R.M. Henson, R.R. Zeyfang, K.V. Kiehl, J. Am. Ceram. Soc. 60 (1977) 15.
- [21] R.R. Zeyfang, R.M. Henson, W.J. Maier, J. Appl. Phys. 48 (1977) 3014.
- [22] Y.Y. Song, H.C. Chen, F.S. Chen, D.L. Sun, P.L. Zhang, W.L. Zhong, J. Syn. Cryst. 18 (1989) 117.
- [23] R.C.R. Franco, E.R. Camargo, M.A.L. Nobre, E.R. Leite, E. Longo, J.A. Varela, Ceram. Int. 25 (1999) 455.

- [24] Y.D. Juang, S.B. Daib, Y.C. Wang, W.Y. Chou, J.S. Hwang, M.L. Hu, W.S. Tse, *Solid State Commun.* 111 (1999) 723.
- [25] Q. Chen, Z. Peng, H. Liu, D. Xiao, J. Zhu, J. Zhu, *J. Am. Ceram. Soc.* 93 (9) (2010) 2788.
- [26] J.H. Shi, W.M. Yang, *J. Alloys Compd.* 472 (2009) 267.
- [27] H. Pan, Y. Hou, X. Chao, L. Wei, Z. Yang, *Curr. Appl. Phys.* 11 (2011) 888.
- [28] E.M. Anton, W. Jo, D. Damjanovic, J. Rodel, *J. Appl. Phys.* 110 (2011) 094108.
- [29] G. Robert, M. Demartin, D. Damjanovic, *J. Am. Ceram. Soc.* 81 (1998) 749.